

DSM extraction and evaluation from Cartosat-1 stereo data for Bhopal city, Madhya Pradesh

Dr. Kakoli Saha

Department of Planning, School of planning and Architecture, Bhopal, Bhopal, 462051, India.

Abstract- Digital surface Models (DSMs) contain information about topographic surfaces and also about other objects higher than the surrounding topographic surface such as buildings, trees etc. therefore, they are ideal for analyzing urban landscape. In this research DSMs of Bhopal city are made from Cartosat 1 stereo data. Three DSMs are made using three different techniques such as adaptive ATE, traditional ATE available through Leica Photogrammetric Suite (LPS) and automated terrain extraction available through Orthoengine. The paper compares the steps of DSM extraction and concluded that process of DSM generation comprised of image orientation and image matching. The output DSMs are compared in context of identifying urban features. It was found that DSM generated through traditional ATE and Orthoengine are more reliable compared to DSM generated through adaptive ATE. This is because; object filter within adaptive ATE modifies the elevation value resulting error in object heights.

Index Terms- Cartosat- 1 stereo data, DSM

I. INTRODUCTION

The term Digital Elevation Model (DEM), digital terrain model (DTM), and Digital Surface Model (DSM) are often incorrectly used as synonyms [6] and a myriad of definitions exist in an attempt to distinguish these terms. It is beyond the realm of this work to disentangle those definitions, but it is commonly accepted that a DSM is a representation of the Earth's surface that includes all objects – both natural and anthropogenic (buildings, trees, power lines etc.). Terrain data portraying elevation information of bare earth can be termed as either DEM or DTM.

DSMs traditionally originating from conventional techniques of pointwise digitising and interpolation have limited capabilities for data manipulation due to labour-intensive efforts to determine arbitrary elevation points; however, there are now a number of sources available for DSM generation. Options range from photogrammetric restitution of stereoscopic aerial and satellite imagery, through airborne laser ranging, commonly termed as lidar, and interferometric synthetic aperture radar (InSAR). In this research, stereo data acquired through Cartosat-1 satellite is used to generate DSM. Several researchers [1, 2, 3, 5, and 9] have generated DSM from Cartosat-1 stereo pairs. Gianinetto [3] calculated DSMs for several test sites of France and concluded that Cartosat-1 proved to be a very good source of data for DSM modeling. Tian et. al. [9]; Crespi et al.[1];and Sirmacek [8] tried to identify buildings from Cartosat generated DSMs. While Crespi et al. [1] generated 3D block models of buildings using

CyberCity-Modeler, Sirmacek et al. [8] , applied a homemade automated approach for building shape detection and Tian et al. [9] used mean-shift segmentation from EDISON library.

In this research, three 5m DSMs are generated from Cartosat1 image. Two of them are generated using traditional Automated Terrain Extraction (ATE) and adaptive ATE in Leica Photogrammetric Suite (LPS) by Erdas Inc. Third DSM is generated using physical model offered by OrthoEngine of Rolta Geomatica Inc. The paper presents a comparative analysis between three different techniques of generating DSM. The outputs (DSMs) are also compared in terms of their applicability to recognize urban features of Bhopal.

II. STUDY AREA

Bhopal city of Madhya Pradesh, India (Fig.1A) is located between 23°09'N and 23°21'N latitude and 77°19'E and 77°31'E longitude. According to 2005 development plan by T&CP, Bhopal, nearly 50% land around the Bhopal city is devoted to residential usage. Besides residential buildings, Bhopal has buildings for commercial, public and semi-public usages. Other categories include industrial, recreational, and transportation (Bhopal Master Plan, 2005). The urban development of Bhopal can be traced back as early as 11th century. Till 2013, the Bhopal municipality area is divided into seventy wards (fig.1B) and covers 285sq.km. area. Since the total municipality boundary covers large area, a smaller test area (ward no.30 covering area of 1.42 sqkm) is selected (fig.1B).

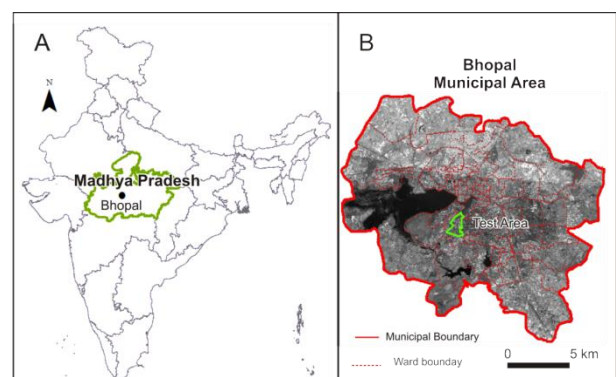


Figure 1. Location map of the study area A. Location of Bhopal. B. Bhopal Municipal area with 70 wards

III. DATA USED

3.1. Satellite imagery

There are two Cartosat-1 scenes which covers the Bhopal Municipal area. Details about the Cartosat scenes are given in the table 1.

Table1. General characteristics of the Cartosat-1 Images used in this study

Product ID	Path	Row	Date of pass	Orbit No	Sun Elevation	Sun Azimuth
132873900401	0532	0290	16 th Feb 2012	36719	47.31	144.35
132873900302	0532	0289	16 th Feb 2012	36719	49.42	141.77

These data sets are provided as Orthokit GeoTiff format and referenced to the WGS84 ellipsoid and datum. Cartosat-1 carries two high-resolution imaging cameras: the afterward looking camera (Aft) and the foreword looking camera (Fore), both the cameras are able to collect panchromatic images with a spatial resolution of 2.5 m on the ground. Thus, each set of data is composed of two images namely band A and band F images. The imaging cameras are fixed to the spacecraft to acquire near-simultaneous imaging of the same scene (with a delay of 52 s between the Fore and the Aft acquisitions) from two different angles: +26° with respect to nadir for the Fore camera and -5° with respect to nadir for the Aft camera.

3.2. Ground Control Points

Six Ground Control Points (GCPs) are collected using a high performance DGPS with about 50 cm horizontal accuracy and 8 m vertical accuracy. The GCPs are acquired with UTM projection and WGS 84 datum. The points are all located on the ground. Those GPS points are well distributed throughout the test area (Fig. 2).

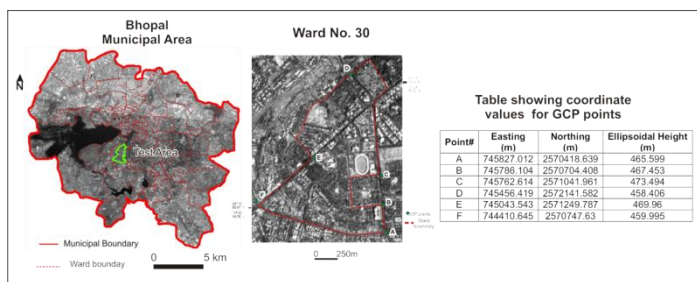


Figure 2. Location of the test area and distribution of GCP points over the test area

IV. METHODOLOGY FOR DSM GENERATION

4.1. Generating DSM in LPS

Leica Photogrammetric Suit (LPS) version 11 software package is used to generate DSM from Cartosat-1 stereo data pairs. As the test area falls within the first scene of table 1 (Product Id 132873900401) only that scene is considered for

further analysis. The method of generating DSM in LPS is described in the flow chart (fig. 3)

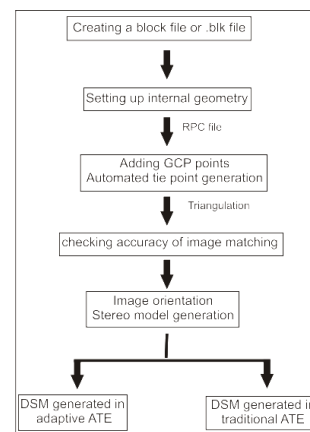


Figure 3. Flow chart showing steps for generating DSM from Cartosat-1 data in LPS

a) Creating block files or .blk files

The process of DSM generation in LPS starts with creating a block project file defining the geometric model as RPC model. Cartosat-1 stereo scenes are provided with Rational Polynomial Coefficient (RPC) within Rational Function (RF) sensor model. The Rational Polynomial Coefficient (RPC) file contains the third degree polynomial coefficients that relate the image to the object space considering the imaging sensor geometry. These RPCs are sensor derived and terrain independent [7]. Rational Polynomial satellite sensor models are simpler empirical mathematical models relating image space (line and column position) to latitude, longitude, and surface elevation. The name Rational Polynomial derives from the fact that the model is expressed as the ratio of two cubic polynomial expressions [4]. The block project has assigned the horizontal and vertical coordinates with UTM projection and WGS 84 datum. The stereo pair images band A and band F (refer section 3.1.) are added to the frame.

b) Setting up internal geometry

The software performs interior and exterior orientation of stereo pairs by extracting information from RPC file. Interior orientation defines the internal geometry of a sensor, as it existed at the time of image capture and exterior orientation is the

position and angular orientation of the sensor that captured the image.

c) Adding GCP points and automated tie point generation

LPS supports both manual and automatic GCP and tie points collection. The software selects a matching point in one image, finding its conjugate point in the other (stereomate) image. During Image Matching in LPS, a correlation window exists on the reference image and a search window exists on the neighbouring overlapping image. The cross-correlation coefficients are calculated for each correlation window among the search window. The correlation coefficient considered as the measure of similarity between the image points appearing within the overlapping areas of image pair. Total 110 tie points are generated in the overlapping area whose ground coordinates are not known. Software use math model to calculate the coordinates of the tie points. In this research the math model is already defined as rational function model (section 4.1.a). Using classical point measurement tool six ground points are added to the images. The X,Y, and Z values for CGP points were provided. Fig.4 shows overlapping images and distribution of tie points and GCP points.

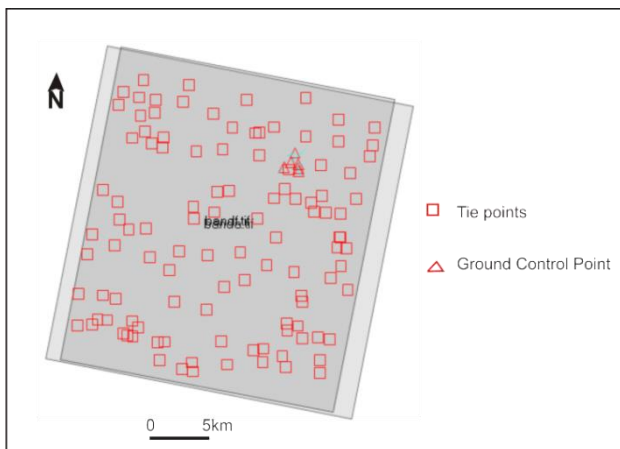


Figure 4. Distribution of tie points and GCP points on overlapping stereo pairs

d) Checking accuracy of the math model

The triangulation was run after adding GCPs and tie points. Triangulation process established relation between images, sensor model and ground points (Krishnamurthy, 2008). Process was run to check the accuracy for GCPs and tie points. The triangulation error report for GCPs is shown in figure 5.

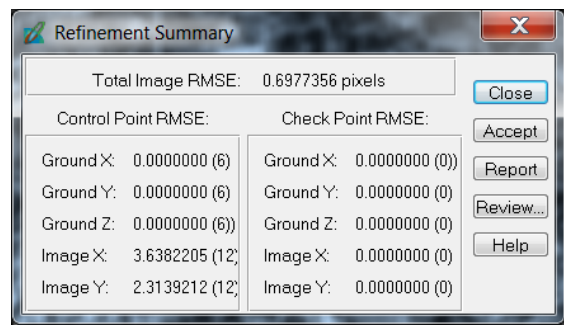


Figure 5. Triangulation error report automatically generated by LPS

In figure 5, the RMSE of total image is 0.6977 pixels. RMSE value below one pixel is the confirmation of the fact that the RF Model is accurate. Elevation values for tie points are then calculated using the math model. The calculated elevation values serve as seed vortices for DSM generation.

e) DSM extraction with traditional ATE

The next phase of the experiment is DSM extraction. Classic Automated Terrain Extraction tool is used for DSM extraction. The output cell size is set to 5m considering the Ground Sampling Distance (GSD) of the original stereo pair is 2.5 m. A recent study described the best resolution as twice the satellite's image pixel size to avoid degradation of the DSM's structure (Gianinetto, 2009). Fig.6B is showing the output DSM generated in traditional ATE.

f) DSM extraction with adaptive ATE

Adaptive ATE, which was introduced to LPS from its 10.1 version uses a global DEM to initialize a surface model and iteratively refines it with image registration on different pyramid levels. Matching results from current pyramid will be used to update terrain range at next lower pyramid (Xu, 2008). Thus the accuracy of matching improves. The global DEM generated with 3-second SRTM DEM. Fig.6.A is showing the DSM extracted with adaptive ATE.

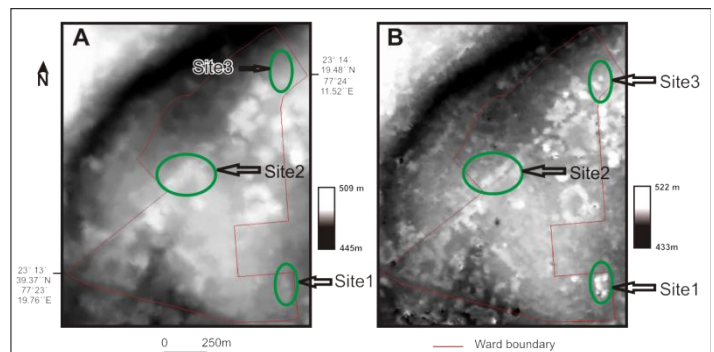


Figure6. A. DSM of the test area generated with adaptive ATE (resolution 5 m); B. DSM of the test area generated with traditional ATE (resolution 5 m).

4.2. Generating DSM in Orthoengine

The steps for generating DSM in Orthoengine by PCI Geomatica is shown in flow chart (fig.7).

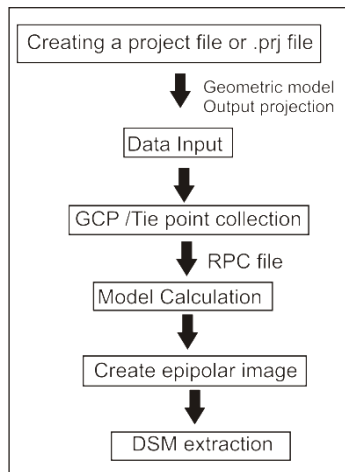


Figure 7.steps for generating DSM in Orthoengine

Fig.7 shows that the orthoengine follows same procedure like LPS to generate DSM. Like LPS Orthoengine also uses same Rational Functions Math Model to calibrate the elevation values for matched points. RPC file is used to perform image orientation and to generate epipolar image. The only difference Orthoengine offers is adjustments in few parameters. For example, unlike LPS it does not allow user to set search window or correlation coefficient (see text in section 4.1.a). The output DSM generated in Orthoengine is displayed in figure 8.

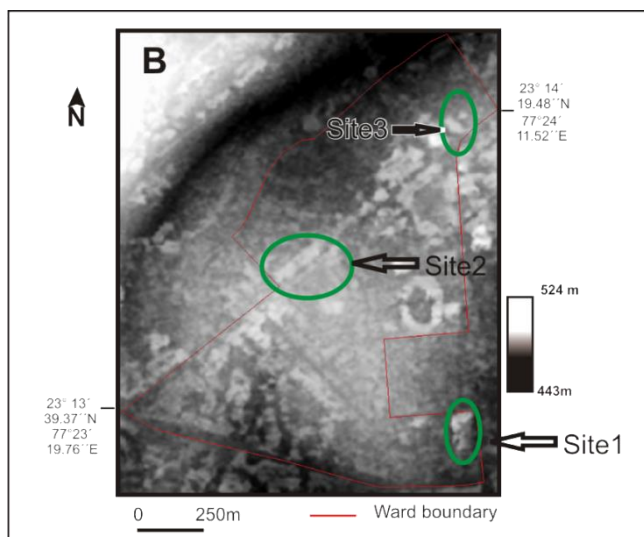


Figure8 . DSM generated in Orthoengine

V. DISCUSSION

5.1 Comparing traditional DSM with adaptive DSM

Urban features specifically buildings are more recognizable in adaptive DSM compared to traditional DSM. To investigate the matter more closely three sites are selected in both the images and building outlines are compared (fig. 6). It is observed that

building edges are sharper in traditional DSM (fig.6B). The reason may be the object filtering used in adaptive ATE. Object filtering is a blunder elimination technique, which removes most spikes as well as points on buildings and trees resulting drop in elevation. As a result, edges of buildings are blurred in adaptive DSM. Also, range of elevation is higher (522m to 433 m) in traditional DSM as compare to adaptive DSM (509m to 445m).

5.2.Comparing Orthoengine generated DSM with other DSMs

Figure 8 shows that urban features, specifically buildings are recognizable in Orthoengine generated DSM. Same three sites have been identified in the DSM and it is found that buildings of those particular sites are recognizable with sharp edges. To investigate the matter more closely the average elevations of buildings of those three sites have been measured in three DSMs. The table 2 shows the measured elevation values.

Table 2: Elevation comparison of same sites between three DSMs

Methods	Elevation in meter		
	Site1	Site2	Site3
Adaptive ATE	477	485	483
Traditional ATE	489	489	492
Orthoengine	488	489	492

Heights of same buildings are significantly low in adaptive DSM compared to DSM generated through traditional ATE and Orthoengine (Table 2).

VI. CONCLUSION

In this research, the process of extracting DSM from Cartosat 1 stereo data is explained. Three different methods offered by two different commercial softwares are used to generate the DSMs. The study area is Bhopal city; the DSMs are compared in context of recognizing urban features. The analysis shows that generation of automated DSM involves image orientation and image matching. Image orientation is performed using information from RPC file. For Cartosat 1 data, RPC file is provided by the vendor. Image matching is performed by identifying matched points in both images of stereo pair and the coordinates of the matched points are calculated using user-defined geometric model. Both softwares uses rational function models to calculate the elevation values for matched points and those values act as seed vortices for DSM generation. The first two DSMs are generated within LPS using adaptive ATE and traditional ATE. From its 10.1 version, LPS is offering adaptive ATE which is an advance algorithm to improve the accuracy of image matching. The third DSM is generated in Orthoengine. The three output DSMs are compared and it is found that urban features such as buildings, roads are more distinct in the DSMs generated through traditional ATE and Orthoengine. On the other hand, in DSM generated through adaptive ATE, the edges of urban features are blurred and therefore hard to recognize. This is because the object filter within adaptive ATE removes the elevation spikes of individual object resulting blur edges for those objects. The modification of elevation also affects the

building elevation. The final conclusion is that the traditional ATE and Orthoengine is preferable over adaptive ATE if the objective of the study is to identify urban features.

ACKNOWLEDGEMENT

The author would like to thank Department of Science and Technology, Government of India for providing funding for this research.

REFERENCES

- [1] Crespi, M., Barbato, F., Vendictis, L.D., Onori, R., Poli, D., Volpe, F., Wang, X., 2008. Orientation, orthorectification, terrain and city modeling from Cartosat-1 stereo imagery: Preliminary results in the first phase of ISPRS-ISRO C-SAP. *Journal of Applied Remote Sensing* 2, pp 023523-023529.
- [2] Dabrowski, R., Jackowski, W.F., Kedzierski, M., Walczykowski, P., Zych, J., 2008. Cartosat-1: orientation, DEM and orthorectification quality assessment, *The International Archives of the Photogrammetry, Remote Sensing and Spatial Information Sciences* Vol. XXXVII. Part B1, pp1309-1313.
- [3] Gianinetto, M., 2009. Evaluation of Cartosat-1 Multi-Scale Digital Surface Modelling Over France, *Sensors* pp 3269-3288.
- [4] Gopala Krishna, B., Amitabh, Srinivasan, T. P., Srivastava, P. K., 2008. DEM generation from high resolution multi-view data product. *The International Archives of the Photogrammetry, Remote Sensing and Spatial Information Sciences* Vol. XXXVII. Part B1. pp 1099-1102
- [5] Kay, S., Zielinski, R., 2006. Orthorectification and geometric quality assessment of Cartosat-1 for common agricultural policy monitoring. *ISPRS* 36, pp. 5.
- [6] Martha, T.R., Kerle, N., Westen, C.V., Jetten, V., Kumar, V., 2010. Effect of Sun Elevation Angle on DSMs Derived from Cartosat-1 Data, *Photogrammetric Engineering & Remote Sensing* 76 (4), pp 429-438.
- [7] Rao, C. V., Sathyanarayana, P., Jain, D. S., Manjunath, A. S., 2007. Topographic map updation using Cartosat-1 data. In *Proceedings of the 2007 Annual Conference of the Remote Sensing & Photogrammetry Society (RSPSoc2007)*, Newcastle upon Tyne. National Remote Sensing Agency.
- [8] Sirmacek, B., Taubenbock, H., Reinartz, P., Ehlers, M., 2012. Performance Evaluation for 3-D City Model Generation of Six Different DSMs From Air- and Spaceborne Sensors, *IEEE Journal of Selected Topics in Applied Earth Observations and Remote Sensing* 5(1), pp 59-70.
- [9] Tian, J., Reinartz, P., d'Angelo, P., Ehlers, M., 2013. Region-based automatic building and forest change detection on Cartosat-1 stereo imagery, *ISPRS Journal of Photogrammetry and Remote Sensing* 79, 226-239.

AUTHORS

First Author – Dr. Kakoli Saha, Ph.D., School of Planning and Architecture Bhopal, Bhopal, Madhya Pradesh, India, kakolisaha@spabhupal.ac.in.

Correspondence Author – Dr. Kakoli Saha, Ph.D., School of Planning and Architecture Bhopal, Bhopal, Madhya Pradesh, India, kakolisaha@spabhupal.ac.in.